

On Precision of the Leptonic Mixing Angle θ_{23} and its Implications for the Flavor Models

S. Cao^{1,*}, P. T. Quyen^{1,2,*}, N. T. Hong Van³, Ankur Nath⁴, and T. V. Ngoc⁵

¹*Institute for Interdisciplinary Research in Science and Education, ICISE, Quy Nhon, Vietnam.*

²*Graduate University of Science and Technology, Vietnam Academy of Science and Technology, Hanoi, Vietnam.*

³*Institute of Physics, Vietnam Academy of Science and Technology, Hanoi, Vietnam.*

⁴*Department of Physics, Namrup College, Assam, India*

⁵*Department of Physics, Kyoto University, Kyoto, Japan*

(Dated: September 19, 2024)

Among three leptonic mixing angles, θ_{23} angle, which characterizes the fractional contribution of two flavor eigenstates ν_μ and ν_τ to the third mass eigenstate ν_3 , is known to be the largest but the least precisely measured. The work investigates possible reach of θ_{23} precision with two upcoming gigantic accelerator-based long-baseline neutrino experiments, namely Hyper-Kamiokande and DUNE experiments as well as a possible joint analyses of future neutrino facilities. Our simulation yields that each experiment will definitely establish the octant of θ_{23} angle for all values within 1σ parameter interval, while considering the current limitation. However, if the actual value is $0.48 \leq \sin^2 \theta_{23} \leq 0.54$, it becomes challenging for these two experiments to reject the maximal ($\theta_{23} = \pi/4$) hypothesis and conclude its octant. This octant-blind region can be further explored with the proposed facilities ESSnuSB and a neutrino factory. Accurate determination of the mixing angle θ_{23} , as well as the accuracy of δ_{CP} , is crucial for examining a certain category of discrete non-Abelian leptonic flavor models. Specifically if CP is conserved in leptonic sector, the combined analysis of Hyper-K and DUNE will rule out the majority of these models. However, if the CP is maximally violated, higher precision of δ_{CP} is necessary for testing these flavor models.

I. CURRENT UNDERSTANDINGS OF NEUTRINO OSCILLATION PARAMETERS

Observation of neutrino oscillation phenomenon [1–3] revolutionizes particle physics at the dawn of the twenty-first century since its implications of massive neutrinos and leptonic mixing are not adequately explained by the Standard Model of elementary particles. The up-to-date data [4], with few anomaly exceptions, can be well-described by a three-flavor neutrino model based on a 3×3 unitary mixing matrix known as Pontecorvo–Maki–Nakagawa–Sakata (PMNS) matrix [5, 6]. The matrix represents the magnitude of the coupling between three neutrino mass eigenstates (ν_1, ν_2, ν_3) and three charged-lepton eigenstates (e, μ, τ). The PMNS matrix is conventionally parameterized by three mixing angles ($\theta_{12}, \theta_{13}, \theta_{23}$), one Dirac CP-violation phase, δ_{CP} , and additional two Majorana CP-violation phases if the neutrinos are Majorana particles. Measurements using neutrino oscillation phenomena, which are not affected by the Majorana phases, enable us to determine the four PMNS oscillation parameters ($\theta_{12}, \theta_{13}, \theta_{23}, \delta_{CP}$) and the neutrino mass-square splittings, represented as $\Delta m_{ij}^2 = m_i^2 - m_j^2$ where $(i, j) = 1, 2, 3$. The neutrino

oscillation measurements typically involve two types of data samples: (i) the survival or *disappearance* of a α -flavor from the neutrino production source, and (ii) the *appearance* of a β -flavor from the α -flavor neutrino production source. The aforementioned process is observed in the survival of ν_e from sun, $\bar{\nu}_e$ from the reactors, $\nu_\mu(\bar{\nu}_\mu)$ from the atmospherics and from accelerator-based source. The *appearance* of $\nu_e(\bar{\nu}_e)$ and $\nu_\tau(\bar{\nu}_\tau)$ from atmospheric and accelerator-based sources of $\nu_\mu(\bar{\nu}_\mu)$ exemplify the later process. The probability of α -flavor neutrinos with energy E transitioning into β -flavor neutrinos observed at a baseline of L in vacuum can be expressed as

$$P(\nu_\alpha \rightarrow \nu_\beta) = \delta_{\alpha\beta} - 4 \sum_{i>j} \Re(U_{\alpha i}^* U_{\beta i} U_{\alpha j} U_{\beta j}^*) \sin^2 \Phi_{ij} \\ \pm 2 \sum_{i>j} \Im(U_{\alpha i}^* U_{\beta i} U_{\alpha j} U_{\beta j}^*) \sin 2\Phi_{ij}$$

where $\Phi_{ij} = \Delta m_{ij}^2 \frac{L}{4E} \equiv 1.27 \times \Delta m_{ij}^2 [\text{eV}^2] \frac{L[\text{km}]}{E[\text{GeV}]}$ and \pm sign is taken for neutrinos and anti-neutrinos, respectively. There are two well-established scales for neutrino mass-squared splittings: $\Delta m_{21}^2 \sim 7.4 \times 10^{-5} \text{ eV}^2/c^4$ and $|\Delta m_{31}^2| \sim 2.5 \times 10^{-3} \text{ eV}^2/c^4$. A crucial point to stress is that the positive or negative nature of Δm_{31}^2 remains unknown at yet. Therefore, it is currently unknown whether neutrino mass spectrum adheres to the *normal* ordering ($m_3 > m_2 > m_1$) or *inverted* ordering ($m_2 > m_1 > m_3$). Experiments T2K [7], NO ν A [8],

* These authors contributed equally to this work.
Corresponding author cvson@ifirse.icise.vn

Parameter	Best fit	3σ C.L. range
$\sin^2 \theta_{12}$	0.303	[0.270, 0.341]
$\sin^2 \theta_{13} (\times 10^{-2})$	2.203	[2.0, 2.4]
$\sin^2 \theta_{23}$	0.572	[0.406, 0.620]
$\delta_{CP} (\circ)$	197	[108, 404]
$\Delta m_{21}^2 (10^{-5} \text{eV}^2/c^4)$	7.41	[6.82, 8.03]
$\Delta m_{31}^2 (10^{-3} \text{eV}^2/c^4)$	2.511	[2.428, 2.597]

TABLE I: Global constraints of neutrino oscillation parameters with *normal* mass ordering assumed, taken from Ref. [16] with NuFit 5.2 based on data available in November 2022.

Super-Kamiokande (Super-K) [9] shows some mild preference to the *normal* mass ordering over the *inverted* one. Combining Higher statistical samples from T2K and NO ν A with the reactor-based medium-baseline experiment JUNO [10] will be crucial for elucidating this unknown [11, 12]. One extra mystery in the PMNS 3-flavor picture is the parameterization-independent amplitude of CP violation, known as leptonic Jarlskog invariance, which is directly related to the CP-violation phase δ_{CP} as

$$J_{CP}^{\text{Lepton}} = \Im[U_{\alpha i} U_{\alpha j}^* U_{\beta i}^* U_{\beta j}] \\ = \frac{1}{8} \sin 2\theta_{12} \sin 2\theta_{23} \sin 2\theta_{13} \cos \theta_{13} \sin \delta_{CP}.$$

The T2K experiment [7, 13] have recently presented a significant hint on the non-zero CP-violation phase. However, NO ν A experiment [8] does not exhibit any similar inclination in the available data. The potential detection of the CP violation before the commencement of the next-generation accelerator-based neutrino experiments Hyper-Kamiokande (Hyper-K) [14] and DUNE [15] make the future joint analysis of T2K and NO ν A [11] a fascinating prospect. The final uncertainty pertains to the proximity of the mixing angle θ_{23} to $\pi/4$. As shown in Table I, the current 3σ C.L. range of $\sin^2 \theta_{23}$ encompasses around 21% of all possible values. The data strongly support the maximal mixing $\theta_{23} = \pi/4$ hypothesis. The near proximity of the mixing angle θ_{23} to maximal is indicative of a hidden symmetry between the second and third elementary particle generations, which are two distinct copies of the irreducible representations of $SU(2)_L$ group. The precise value of θ_{23} would be an important input to the flavor and neutrino mass models, as illustrated in Ref. [17, 18] and references therein.

This Letter aims to provide a concise overview of the uncertainty associated with measuring the θ_{23} mixing angle, estimate the possible reach of θ_{23} , and analyze its implications for a certain category of flavor models.

II. AMBIGUITY IN MEASURING THE θ_{23} MIXING ANGLE

The current knowledge of θ_{23} is mostly derived from neutrino oscillation measurements conducted using two sources: (i) atmospheric neutrinos and (ii) accelerator-based neutrinos. Joint analysis of accelerator-based and atmospheric neutrino sources in MINOS and MINOS+ experiments [19] revealed $\sin^2 \theta_{23} = 0.43^{+0.20}_{-0.04}$, which is consistent with maximal mixing hypothesis at 1σ C.L. Measurement using the atmospheric neutrino data from Super-K [20] yields an interval of $0.41 \leq \sin^2 \theta_{23} \leq 0.58$ at the 90% C.L. Both current data from accelerator-based long-baseline T2K [7] and NO ν A [8] favor slightly the upper octant of the mixing angle θ_{23} . The current global fit data [16] using NuFit 5.2 supports the maximal mixing hypothesis at 90% C.L.. The measurements from leading experiments and the global analysis of neutrino oscillation measurements are summarized in Table II. In long-baseline experiments using accelerator-based neutrino sources like ongoing T2K [24], and NO ν A [25], and upcoming Hyper-K [14] and DUNE [15], the precise θ_{23} value can be extracted from a measurement of ν_μ -survival probability ($P(\nu_\mu \rightarrow \nu_\mu)$, $P(\bar{\nu}_\mu \rightarrow \bar{\nu}_\mu)$ or called as *disappearance* samples) and/or *appearance* of electron neutrinos from produced muon neutrinos ($P(\nu_\mu \rightarrow \nu_e)$, $P(\bar{\nu}_\mu \rightarrow \bar{\nu}_e)$ and known as *appearance* samples). Eq. (1) describes the survival probability of muon neutrinos around the oscillation maximum $\Phi_{31} \equiv 1.27 \times \Delta m_{31}^2 [\text{eV}^2] \frac{L[\text{km}]}{E[\text{GeV}]} \approx \pi/2$, which is applicable to T2K, NO ν A, and Hyper-K experimental setups.

$$P_{\nu_\mu \rightarrow \nu_\mu} (\Phi_{31} \approx \pi/2) \\ = 1 - (\cos^4 \theta_{13} \sin^2 2\theta_{23} + \sin^2 2\theta_{13} \sin^2 \theta_{23}) \sin^2 \Phi_{31} \\ + \epsilon_m \Phi_{31} \sin 2\Phi_{31} (\cos^2 \theta_{12} \sin^2 2\theta_{23} - \sin^2 \theta_{23} J_{123} \cos \delta_{CP}), \quad (1)$$

where $\epsilon_m = \frac{\Delta m_{21}^2}{\Delta m_{31}^2}$ and $J_{123} = \sin 2\theta_{12} \sin 2\theta_{23} \sin 2\theta_{13}$. The leading order term of Eq. (1) reveals that the survival probability reaches its minimum at approximately $\sin^2 \theta_{23} \approx 0.5 \cos^{-2} \theta_{13} = 0.51$, given $\sin^2 \theta_{13} = 0.022$. The survival oscillation probability $P_{\nu_\mu \rightarrow \nu_\mu}$ exhibits symmetry at this point and results in a discrete octant degeneracy: two discrete values of $\sin^2 \theta_{23}$ correspond to identical probabilities. Furthermore, when a truth value of $\sin^2 \theta_{23}$ is found in lower octant or $\sin^2 \theta_{23} > 0.52$, one always finds a wrong-octant solution if the *disappearance* sample is used. When $\sin^2 \theta_{23}$ is in higher octant but smaller than 0.52, the continuous degeneracy is also observed in the same octant.

To overcome the octant degeneracy in the *disappearance* channel, one approach is to utilize the sample of *appearance* data. Eq. (2) provides the approximate ν_e *appearance* probability around the oscillation maximum

	T2K	NO ν A	MINOS	Super-K	IceCube	NuFIT 5.2
Best fit $\sin^2 \theta_{23}$	$0.561^{+0.019}_{-0.038}$	$0.57^{+0.03}_{-0.04}$	$0.43^{+0.20}_{-0.04}$	$0.425^{+0.051}_{-0.034}$	0.51 ± 0.05	$0.572^{+0.018}_{-0.023}$
Maximal rej. [σ]	1.22	1.29	0.90	1.25	0.28	1.69
Wrong-octant rej. [σ]	1.22	0.37	0.53	0.85	0	0.89
Constrained $\sin^2 \theta_{13}/10^{-2}$	2.18 ± 0.07	2.10 ± 0.11	2.10 ± 0.11	2.10 ± 0.11	2.224 ± 0.11	2.203 ± 0.0575

TABLE II: Current constraints on $\sin^2 \theta_{23}$ from T2K [7], NO ν A [21], MINOS(+) [19], Super-K [22], IceCube [23] and NuFIT 5.2 [16] with a *normal* mass ordering assumed.

$\Phi_{31} \approx \pi/2$ in vacuum.

$$P_{\nu_\mu \rightarrow \nu_e} (\Phi_{31} \approx \pi/2) = \sin^2 \theta_{23} \sin^2 2\theta_{13} \sin^2 \Phi_{31} + \epsilon_m \Phi_{31} \sin \Phi_{31} J_{123} \cos(\Phi_{31} - \delta_{CP}), \quad (2)$$

The leading term of the ν_e *appearance* probability is determined by the factor $\sin^2 \theta_{23}$, making it highly responsive to the octant of θ_{23} . In addition, Eq. (2) shows that the magnitude of this flavor transition is modulated by both the poorly-established δ_{CP} and unknown neutrino mass ordering. Nevertheless, when both ν_e *appearance* and $\bar{\nu}_e$ *appearance* are measured with rather high statistical significance, the octant resolving has a marginal influence of the actual value of δ_{CP} . Besides, it is found that the relative difference in the probabilities of the ν_e ($\bar{\nu}_e$ *appearance*) between the *normal* and *inverted* mass ordering is largely unaffected by the actual value of $\sin^2 \theta_{23}$ but only the true value of δ_{CP} . Consequently, the precision measurement of θ_{23} does not depend significantly on the neutrino mass ordering.

A relevant parameter which significantly influences the determination of the θ_{23} octant in case of non-maximal mixing is the precision value of θ_{13} . While the observation of $\nu_\mu \rightarrow \nu_e$ transition by T2K [26] established the non-zero value of θ_{13} , the most accurate measurement of this mixing angle is obtained from the reactor-based experiments [4]. From Eq. (2), the analytical formula to describe the continuous degeneracy between θ_{23} and θ_{13} can be formulated as

$$\sin 2\theta_{13}^{\text{true}} \sin \theta_{23}^{\text{true}} = \sin 2\theta_{13}^{\text{cloned}} \sin \theta_{23}^{\text{cloned}},$$

where $(\theta_{13}^{\text{true}}, \theta_{23}^{\text{true}})$ are true values while $(\theta_{13}^{\text{cloned}}, \theta_{23}^{\text{cloned}})$ are cloned solutions for a given $\nu_\mu \rightarrow \nu_e$ probability. This degeneracy suggests that the precision of the later will have a significant impact on the precision, as well as the octant resolving, of the former. Indeed, the effect has been observed in T2K data [7] where the data with and without reactor constraint on θ_{13} exhibits different preference for octant of θ_{23} . The reason is that T2K data itself favor a greater value of θ_{13} than the stringent constraint obtained from the reactor-based measurements. We provide a summary of the possible measurements in Fig. 1, which are displayed on the parameter space of θ_{23} - θ_{13} , in order to clarify the uncertainty in determining the mixing angle θ_{23} . For illustrative purpose, the true value of $\sin^2 \theta_{23}$ is set at 0.6 and $\sin^2 \theta_{13}$ is set at 0.022. Using measurement with the $\nu_\mu \rightarrow \nu_\mu$ data channel, two

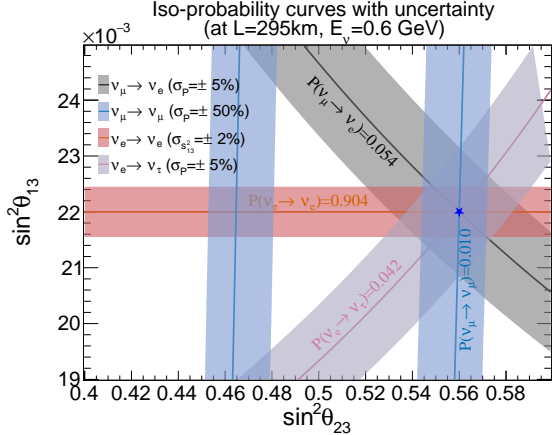


FIG. 1: Schematic view of addressing the ambiguity of θ_{23} is presented with the iso-probability curves in the $(\sin^2 \theta_{23}, \sin^2 \theta_{13})$ parameter space. The error band for each curve is obtained with a predefined uncertainty of probability σ_p . This includes $\nu_\mu \rightarrow \nu_\mu$, $\nu_\mu \rightarrow \nu_e$, $\nu_\mu \rightarrow \nu_\tau$, and $\nu_e \rightarrow \nu_e$ transitions. The true values of parameters are set to $\sin^2 \theta_{23}=0.6$ and $\sin^2 \theta_{13}=0.02204$ from NuFIT 5.2.

distinct solutions will be obtained, one of which will be cloned in the lower octant. The curves of $\nu_\mu \rightarrow \nu_e$ and $\nu_e \rightarrow \nu_\tau$ iso-probability are orthogonal since the leading term of the probability is proportional to $\sin^2 \theta_{23} \sin^2 2\theta_{13}$ for the former and as $\cos^2 \theta_{23} \sin^2 2\theta_{13}$ for the later. Measurements made using $\nu_e \rightarrow \nu_e$ or $\bar{\nu}_e \rightarrow \bar{\nu}_e$ is marginally sensitive to θ_{23} but they are crucial for accurately measuring the θ_{13} value and hence valuable for resolving the octant of θ_{23} in case of non-maximal mixing. Recent measurements [16] have yielded a precision of 2.6% on $\sin^2 \theta_{13}$, corresponding to 1.3% uncertainty of θ_{13} . Furthermore, the value of $\sin^2 \theta_{13}$ can be improved to 1% (or 0.5% uncertainty of θ_{13}) [27]. The θ_{23} sensitivity will be calculated using these two constraints.

It is important to point out that the primary purpose of the θ_{23} measurements is to quantitatively assess the proximity of θ_{23} to the maximal mixing. This, as discussed in Sec. IV, has considerable implications for testing the flavor models. From an empirical standpoint, this entails two consecutive hypothesis tests: (i) excluding the maximal mixing, and (ii) identifying the octant if non-maximal mixing is detected. The former can be

Exp.	Octant-blind regions of $\sin^2 \theta_{23}$	
	3σ C.L.	5σ C.L.
T2HK	[0.47, 0.55]	[0.45, 0.57]
DUNE	[0.47, 0.56]	[0.44, 0.58]
ESSnuSB	[0.46, 0.56]	[0.43, 0.58]
Nu-Factory	[0.48, 0.53]	[0.47, 0.59]

TABLE III: The octant-blind region at 3σ and 5σ C.L. of θ_{23} with individual T2HK and DUNE, ESSnuSB, and Neutrino Factory. Here current constraint of θ_{13} is used.

quantitatively evaluated using statistics at a given θ_{23}^t in the vector of relevant parameter $\vec{\sigma}$:

$$\Delta\chi^2_1(\vec{\sigma}; \theta_{23}^t) = \chi^2_{\min.}(\vec{\sigma}; \theta_{23} = \pi/4) - \chi^2_{\min.}(\vec{\sigma}; \theta_{23}^{\text{b.f.}})$$

where $(\vec{\sigma}; \theta_{23}^{\text{b.f.}})$ is the best-fit parameter vector, which ideally equals to $\vec{\sigma}$ and $\theta_{23}^{\text{b.f.}} = \theta_{23}^t$. The statistical measure for the latter problem is defined as the relative difference of χ^2 between the true-octant (T.O.) and the wrong-octant (W.O.) in the θ_{23} parameter space:

$$\Delta\chi^2_2(\vec{\sigma}; \theta_{23}^t) = \chi^2_{\min.}(\vec{\sigma}; \theta_{23}^{\text{b.f.}} \text{ in W.O.}) - \chi^2_{\min.}(\vec{\sigma}; \theta_{23}^{\text{b.f.}} \text{ in T.O.})$$

Due to the continuity of the neutrino oscillation probability as function of θ_{23} , the statistical significance to exclude the maximal mixing is greater than that of excluding the wrong-octant. In the long-baseline accelerator-based experiments, the $\nu_\mu \rightarrow \nu_\mu$ disappearance sample is the more significant data sample for addressing the first hypothesis test, unless the actual $\sin^2 \theta_{23}$ exhibits a small deviation from the maximal mixing towards the higher octant. In contrast, the $\nu_\mu \rightarrow \nu_e$ appearance sample is crucial for resolving octants in case of non-maximal mixing.

III. PRECISION MEASUREMENT OF θ_{23} ANGLES

We utilize the GloBES software [28, 29] to evaluate the sensitivity of neutrino experiments to the θ_{23} precision. The configuration of each experiment has been revised to make it compatible with the technical design reports of T2HK [14], DUNE [15, 30], ESSnuSB [31], and the neutrino factory [32, 33]. Octant-blind region for a given statistical significance is defined as the range of $\sin^2 \theta_{23}$ where the octant cannot be definitively determined if the true value lies within. The expected octant-blind region of the future neutrino experiments are shown in Table III. Both T2HK and DUNE experiments would be able to resolve the octant of mixing angle θ_{23} at 3σ C.L. if the true value of $\sin^2 \theta_{23}$ lies outside of the [0.47, 0.56] range. The proposed ESSnuSB is capable of accessing a slightly narrower region of θ_{23} . In neutrino factory, it is possible to investigate a wider range of mixing angle θ_{23} in both octants.

The numbers presented in Table III are calculated based on the existing limitations of the leptonic mixing parameters. An estimation using a 1% uncertainty on the

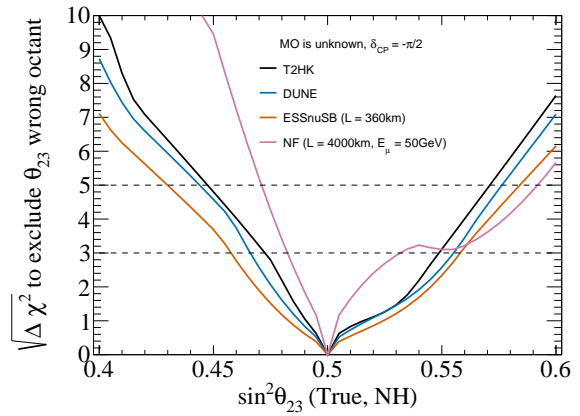


FIG. 2: The statistical significance to exclude the wrong-octant as function of $\sin^2 \theta_{23}$ with different experiments. Here $\delta_{CP} = -\pi/2$ is set, neutrino mass ordering (MO) is presumably unknown, and other relevant parameters and their uncertainties are take from Table I.

Joint analysis	Octant-blind region of $\sin^2 \theta_{23}$	
	3σ C.L.	5σ C.L.
T2HK	[0.47, 0.55]	[0.45, 0.57]
+ DUNE	[0.48, 0.54]	[0.46, 0.56]
+ improved (θ_{13}, θ_{12})	[0.48, 0.54]	[0.47, 0.55]
+ ESSnuSB	[0.48, 0.53]	[0.47, 0.55]
+ Neutrino Factory	[0.49, 0.52]	[0.48, 0.54]

TABLE IV: Octant-blind region at 3σ and 5σ C.L. of θ_{23} with staging joint analyses

$\sin^2 \theta_{13}$ reveals that the 3σ C.L. octant blind region can be narrowed down by less than 10%. More precisely, the percentage is around 8% for T2HK, 5% for DUNE and 9% considering a combined analysis of T2HK and DUNE. While the precision of θ_{12} can achieve sub-percent accuracy with JUNO [34], its effect on the precision of θ_{23} is minimal. Nevertheless, this unprecedented θ_{12} constraint serves to narrow down the allowed range of parameters predicted by the flavor models outlined in Section IV, allowing data to differentiate the models.

Our simulation, depicted in Fig. 3, suggests that T2HK and DUNE will conclusively establish the higher octant of θ_{23} for all values of θ_{23} within the currently fitted $\pm 1\sigma$ interval of parameter. However, if the actual value of $\sin^2 \theta_{23}$ falls within the range of [0.48, 0.54], its ambiguity can not be solved definitively with a statistical significance of 3σ C.L. or higher, even with the use of T2HK, DUNE, or their joint analysis with envisaged constraint on θ_{13} and θ_{12} . In this scenario, possible solution to enhancing the reach of θ_{23} is to do a combined analysis of the T2HK and DUNE with the proposed ESSnuSB and Neutrino Factory. As shown in Fig. 3 and reported in Table. IV, the octant ambiguity at 3σ C.L. can be resolved if the truth value of $\sin^2 \theta_{23}$ lies outside of [0.49, 0.52].

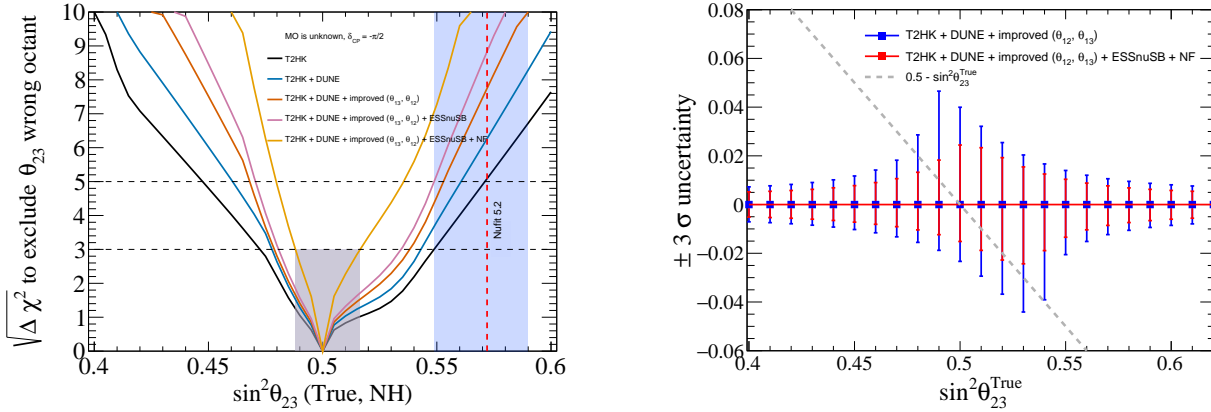


FIG. 3: The left plot presents statistical significance to exclude the wrong-octant as function of $\sin^2 \theta_{23}$ with T2HK and various configuration of joint analyses. The right is the $\pm 3\sigma$ uncertainty as function of true value of $\sin^2 \theta_{23}$ with joint analyses. Here $\delta_{CP} = -\pi/2$ is set, MO is presumably unknown.

IV. IMPLICATION FOR THE LEPTONIC FLAVOR MODELS

That leptonic mixing, represented by two relatively large angles $\theta_{23} \approx \pi/4$, $\theta_{12} \approx \pi/6$, and small angle $\theta_{13} \approx \pi/20$ in the PMNS matrix, is so different from the quark mixing, expressed by approximate unity CKM matrix, triggers questions whether the underlying symmetry is responsible for such patterns and how to describe them in a unified framework. Apparently, the question is relevant to unknown nature of neutrino mass. In this analysis, we examine a category of theoretical models in which the leptonic mixing matrix arises from the misalignment between the *flavor-definite* states $\{l_\alpha, \nu_\alpha\}$ and *symmetry* states $\{\tilde{l}_\alpha, \tilde{\nu}_\alpha\}$ of both charged and neutral leptons [17]. The weak charged-current is written as $J_\mu = \tilde{l} \gamma^\mu (1 - \gamma_5) \tilde{\nu} \equiv \tilde{l} \gamma^\mu (1 - \gamma_5) U_l^\dagger U_\nu \nu$ resulting in a formulation $U_{\text{PMNS}} = U_l^\dagger U_\nu$ where U_l and U_ν are unitary transformation matrices which rotate the states: $\tilde{l} = U_l l$ and $\tilde{\nu} = U_\nu \nu$; and diagonalize the mass matrices $U_l^\dagger M_l M_l^\dagger U_l = \text{diag}(m_e^2, m_\mu^2, m_\tau^2)$ and $U_\nu^\dagger M_\nu U_\nu = \text{diag}(m_1, m_2, m_3)$. The mass matrices of charged and neutral leptons are assumed to be invariant when subjected to non-Abelian discrete symmetries G_l and G_ν respectively, which were commonly originated from a family symmetry G_f , see [35, 36] and references therein. Several $\{G_f \rightarrow G_l \oplus G_\nu\}$ models have been proposed to examine whether the hypothetical patterns of the leptonic mixing agrees with the measured neutrino parameters or not. Among them, the class of flavor models that involve the predictability of the less known δ_{CP} based on its relationship with other more precisely constrained mixing angles is of noteworthy interest because of its testability. The so-called *solar* sum rules [37], in which U_ν is characterized by a maximal $\theta_{23}^\nu = \pi/4$ rotation in 2-3 generation plane, a predetermined θ_{12}^ν in 1-2 generation plane, and non-diagonal U_l to account for rel-

atively small of the θ_{13} angle, establish following relation:

$$\cos \delta_{CP} = \frac{\tan \theta_{23}}{\sin 2\theta_{12} \sin \theta_{13}} [\cos 2\theta_{12}^\nu + (\sin^2 \theta_{12} - \cos^2 \theta_{12}^\nu)(1 - \cot^2 \theta_{23} \sin^2 \theta_{13})]. \quad (3)$$

The value of $\sin \theta_{12}^\nu$ are fixed at (i) $1/\sqrt{2}$, (ii) $1/\sqrt{3}$, (iii) $1/2$, (iv) $1/\sqrt{\sqrt{5}r_g}$ with golden ratio $r_g = (1 + \sqrt{5})/2$, (v) $\sqrt{3 - r_g}/2$, (vi) $\sqrt{(2 - r_g)/3}$ depending on the symmetry form of the U_ν matrices, which are, respectively, (i) bi-maximal (BM), (ii) tri-bimaximal (TBM), (iii) hexagonal (HG), (iv) golden rule type A (GRA), (v) golden rule type B (GRB), and (vi) golden rule type C (GRC). Eq. (3) exhibits a non-negligible dependence of δ_{CP} on the θ_{23} , particularly deviation of $\cos \delta_{CP}$ from zero is greater as the value of θ_{23} increases. It is observed that the BM and GRC models are disfavored since a valid δ_{CP} acquires θ_{23} to be out of the current 3σ C.L. allowed range of this parameter. The remaining four models predict significant amount of the CP violation. Alternative models, in which U_l is assumed to be diagonal and symmetry pattern of U_ν to be partially broken to formulate empirically the observed PMNS matrix, have also been investigated [38]. There are two *atmospheric* sum rules, known as TM1 and TM2, depending on the first or second column of the tri-bimaximal form of U_ν kept to be conserved. TM1 and TM2 establish a relation between θ_{12} and θ_{13} mixing angles, specified as $\sin^2 \theta_{12} = \frac{1 - 3 \sin^2 \theta_{13}}{3(1 - \sin^2 \theta_{13})}$ and $\sin^2 \theta_{12} = \frac{1}{3(1 - \sin^2 \theta_{13})}$ respectively. The predictions are consistent in 3σ C.L. with the current constraint of oscillation parameters shown in Table I. These predictions will be further tested by future neutrino experiments, when the precision of both θ_{12} and θ_{13} mixing angle will be improved. Moreover, TM1 and TM2 enforce a relationship between δ_{CP} and other mixing parameters,

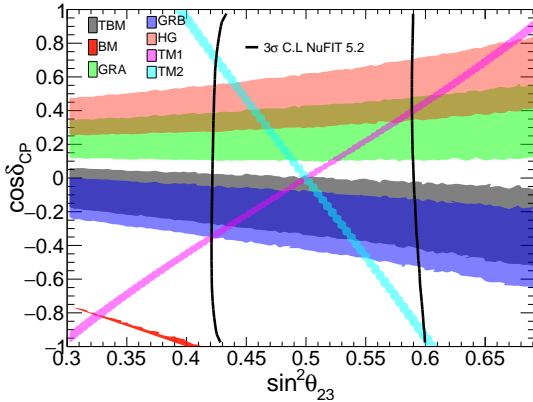


FIG. 4: Allowed parameter spaces in $(\delta_{CP}, \theta_{23})$ with flavor models is overlaid with current constraint of the global neutrino data.

provided in Eq. (4).

$$\cos \delta_{CP} = \begin{cases} -\frac{(1-5 \sin^2 \theta_{13}) \cot 2\theta_{23}}{2\sqrt{2} \sin \theta_{13} \sqrt{1-3 \sin^2 \theta_{13}}} & (\text{TM1}) \\ \frac{(1-2 \sin^2 \theta_{13}) \cot 2\theta_{23}}{\sin \theta_{13} \sqrt{2-3 \sin^2 \theta_{13}}} & (\text{TM2}) \end{cases} \quad (4)$$

In comparison to the *solar* sum rules, the *atmospheric* sum rules exhibit a more pronounced correlation between the value of δ_{CP} and the value of θ_{23} . The allowed parameter space in $(\delta_{CP}, \theta_{23})$ of the above-mentioned flavor models are presented in Fig. 4. Given the current 3σ C.L. range of $\sin^2 \theta_{23}$, all models, with the exception of the BM and GRB which are not consistent with data, predict a substantial violation of the CP symmetry in the lepton sector. The differential among *solar* sum rules are relatively small due to the uncertainty on θ_{12} and θ_{13} . Fig. 5 shows the allowed parameter space in $(\delta_{CP}, \theta_{23})$ of the flavor models, assuming that the central values of $\sin^2 \theta_{12}$ and $\sin^2 \theta_{13}$ remain unchanged, but their uncertainty is decreased to 0.5% and 1.0% respectively. In comparison to Fig. 4, the predicted parameter spaces from different *solar* sum rules become more distinguishable, thereby enhancing the test capability. We find that if CP is conserved, a joint of T2HK and DUNE would be sensitive enough to eliminate all *solar* and *atmospheric* TM1 sum rule for all possible allowed value of θ_{23} . The CP conservation is still applicable for TM2 if θ_{23} is significantly deviated from the maximal mixing, specifically when actual value of $\sin^2 \theta_{23}$ is close to 0.4 in lower octant or 0.6 in higher octant. Thus the measurement of θ_{23} (in addition to θ_{12}) measurement will settle the test for TM2. For maximum CP violation ($\cos \delta_{CP} = 0$), we find that uncertainty of $\cos \delta_{CP}$ of T2HK and DUNE, which is around the range of [-0.5, 0.6] at 3σ C.L., is not sufficient for differentiating the *solar* and *atmospheric* TM1 sum rule. If actual $\sin^2 \theta_{23}$ fall outside of [0.44, 0.56], the analysis will rule out the *atmospheric* TM2 sum rule. Fig. 5 includes a possibility of $\cos \delta_{CP} - \sin^2 \theta_{23}$ sensitivity us-

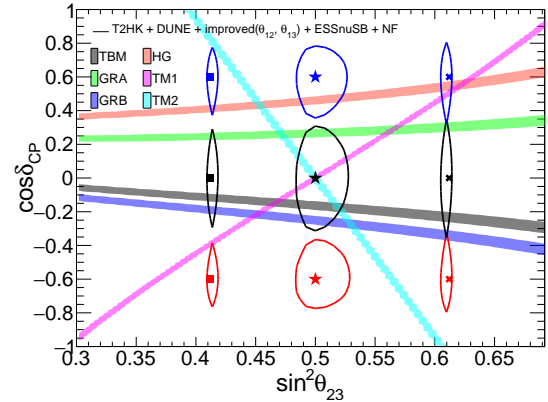


FIG. 5: The allowed parameter space in $(\delta_{CP}, \theta_{23})$ with flavor models is tightened when applying more precise measurement of θ_{13} , θ_{12} . The sensitivity contours of future constraints at some actual values of parameter are computed with joint analysis of simulated data using T2HK, DUNE, ESSnuSB and Neutrino Factory.

ing a combined T2HK, DUNE, ESSnuSB and Neutrino Factory. it is found that this ultimate analysis, which can achieve precision of $\cos \delta_{CP}$ around the range of [-0.26, 0.30], will rule out the *solar* HG sum rule in entire parameter space of θ_{23} . Also, the enhancement in the $\cos \delta_{CP}$ precision also help to eliminate the *atmospheric* TM1 and TM2 models if $\sin^2 \theta_{23}$ is found to be out of the range of [0.44-0.57] and [0.47,0.53] respectively. However, the sensitivity of this ultimate reach on $\cos \delta_{CP}$ is not sufficient to distinguish the *solar* TBM, GRA, GRB sum rules.

V. SUMMARY

The present landscape of the neutrino oscillation measurement indicates that θ_{23} is in close proximity to the maximal mixing. We explore the optimum extent of this mixing angle by analysis of forthcoming influential experiments, Hyper-K and DUNE with potential future inclusion of ESSnuSB and the neutrino factory. Our findings indicate that the accuracy of this measurement does not depend significantly on the truth value as well as the precision of δ_{CP} . Furthermore, it is not affected by the unidentified neutrino mass ordering. As long as the actual value falls within the current $\pm 1\sigma$ interval, both Hyper-K and DUNE can assert the higher octant of θ_{23} . However, if the value of θ_{23} is within the octant-blind region of [0.48,0.54] at 3σ C.L., these experiments cannot resolve the ambiguity of this parameter. A possible solution is to have a joint analysis with ESSnuSB and Neutrino Factory, provided that the data is available. Within this scenario, the octant-blind region will be narrowed down to a range of [0.49,0.52]. The precision measurement of θ_{23} , together with the δ_{CP} precision, is essential for test-

ing a category of flavor models that result in an exact relationship between these two parameters via the *solar* and *atmospheric* sum rules. We find that if CP is conserved, Hyper-K and DUNE will eliminate nearly all of these models. In the case that the CP is maximally violated, only *atmospheric* TM2 can be excluded if real value of θ_{23} is significantly deviated from $\pi/4$. Conducting a combined analysis with ESSnuSB and Neutrino factory, if available, can effectively eliminate the *solar* HG sum rules and both *atmospheric* TM1 and TM2 sum rules in certain range of θ_{23} . Nevertheless, the overall sensitivity is inadequate to tell preference of data to particular *solar*

sum rule model among TBM, GRA, and GRB models.

ACKNOWLEDGEMENT

S. Cao would like to thank KEK for their hospitality during his visit. A. Nath wishes to express gratitude to IFIRSE, ICISE for their hospitality. Phan To Quyen was funded by the Master, PhD Scholarship Programme of Vingroup Innovation Foundation (VINIF), code VINIF.2023.TS.095. The research of S. Cao and N. T. H. Van is funded by the National Foundation for Science and Technology Development (NAFOSTED) of Vietnam under Grant No. 103.99-2023.144.

[1] Y. Fukuda *et al.* (Super-Kamiokande Collaboration), “Evidence for oscillation of atmospheric neutrinos,” *Phys. Rev. Lett.* **81**, 1562 (1998), arXiv:hep-ex/9807003.

[2] Q. Ahmad *et al.* (SNO Collaboration), “Measurement of the rate of $\nu_e + d \rightarrow p + p + e^-$ interactions produced by 8B solar neutrinos at the Sudbury Neutrino Observatory,” *Phys. Rev. Lett.* **87**, 071301 (2001), arXiv:0106015 [nucl-ex].

[3] Q. Ahmad, R. Allen, T. Andersen, J. Anglin, J. Barton, E. Beier, M. Bercovitch, J. Bigu, S. Biller, R. Black, *et al.*, “Measurement of day and night neutrino energy spectra at sno and constraints on neutrino mixing parameters,” *Phys. Rev. Lett.* **89**, 011302 (2002).

[4] S. Navas *et al.* (Particle Data Group), “Review of particle physics,” *Phys. Rev. D* **110**, 030001 (2024).

[5] B. Pontecorvo, “Neutrino experiments and the problem of conservation of leptonic charge,” *Sov. Phys. JETP* **26**, 165 (1968).

[6] Z. Maki, M. Nakagawa, and S. Sakata, “Remarks on the unified model of elementary particles,” *Prog. Theor. Phys.* **28**, 870 (1962).

[7] K. Abe *et al.* (T2K), “Measurements of neutrino oscillation parameters from the T2K experiment using 3.6×10^{21} protons on target,” *Eur. Phys. J. C* **83**, 782 (2023), arXiv:2303.03222 [hep-ex].

[8] M. Acero, P. Adamson, L. Aliaga, N. Anfimov, A. Antoshkin, E. Arrieta-Diaz, L. Asquith, A. Aurisano, A. Back, C. Backhouse, *et al.*, “Improved measurement of neutrino oscillation parameters by the nova experiment,” *Physical Review D* **106**, 032004 (2022).

[9] T. Wester *et al.* (Super-Kamiokande), “Atmospheric neutrino oscillation analysis with neutron tagging and an expanded fiducial volume in Super-Kamiokande I–V,” *Phys. Rev. D* **109**, 072014 (2024), arXiv:2311.05105 [hep-ex].

[10] Z. Djurcic *et al.* (JUNO Collaboration), “JUNO Conceptual Design Report,” (2015), arXiv:1508.07166 [physics.ins-det].

[11] S. Cao, A. Nath, T. V. Ngoc, P. T. Quyen, N. T. Hong Van, and N. K. Francis, “Physics potential of the combined sensitivity of T2K-II, NO ν A extension, and JUNO,” *Phys. Rev. D* **103**, 112010 (2021), arXiv:2009.08585 [hep-ph].

[12] A. Cabrera *et al.*, “Synergies and prospects for early resolution of the neutrino mass ordering,” *Sci. Rep.* **12**, 5393 (2022), arXiv:2008.11280 [hep-ph].

[13] K. Abe *et al.* (T2K), “Constraint on the matter–antimatter symmetry-violating phase in neutrino oscillations,” *Nature* **580**, 339 (2020), [Erratum: *Nature* 583, E16 (2020)], arXiv:1910.03887 [hep-ex].

[14] K. A. Hyper-Kamiokande Proto-Collaboration, *et al.*, “Hyper-kamiokande design report,” (2018), arXiv:1805.04163 [physics.ins-det].

[15] B. Abi *et al.* (DUNE), “Deep Underground Neutrino Experiment (DUNE), Far Detector Technical Design Report, Volume I Introduction to DUNE,” *JINST* **15**, T08008 (2020), arXiv:2002.02967 [physics.ins-det].

[16] I. Esteban, M. C. Gonzalez-Garcia, M. Maltoni, T. Schwetz, and A. Zhou, “The fate of hints: updated global analysis of three-flavor neutrino oscillations,” *JHEP* **09**, 178 (2020), arXiv:2007.14792 [hep-ph].

[17] R. N. Mohapatra and A. Y. Smirnov, “Neutrino Mass and New Physics,” *Ann. Rev. Nucl. Part. Sci.* **56**, 569 (2006), arXiv:hep-ph/0603118.

[18] J. Gehrlein, S. Petcov, M. Spinrath, and A. Titov, “Testing neutrino flavor models,” in *Snowmass 2021* (2022) arXiv:2203.06219 [hep-ph].

[19] P. Adamson *et al.* (MINOS+), “Precision Constraints for Three-Flavor Neutrino Oscillations from the Full MINOS+ and MINOS Dataset,” *Phys. Rev. Lett.* **125**, 131802 (2020), arXiv:2006.15208 [hep-ex].

[20] R. Wendell *et al.* (Super-Kamiokande), “Atmospheric neutrino oscillation analysis with sub-leading effects in Super-Kamiokande I, II, and III,” *Phys. Rev. D* **81**, 092004 (2010), arXiv:1002.3471 [hep-ex].

[21] M. A. Acero *et al.* (NO ν A), “Improved measurement of neutrino oscillation parameters by the NO ν A experiment,” *Phys. Rev. D* **106**, 032004 (2022), arXiv:2108.08219 [hep-ex].

[22] M. Jiang *et al.* (Super-Kamiokande), “Atmospheric Neutrino Oscillation Analysis with Improved Event Reconstruction in Super-Kamiokande IV,” *PTEP* **2019**, 053F01 (2019), arXiv:1901.03230 [hep-ex].

[23] R. Abbasi *et al.* ((IceCube Collaboration)*, IceCube), “Measurement of atmospheric neutrino mixing with improved IceCube DeepCore calibration and data processing,” *Phys. Rev. D* **108**, 012014 (2023), arXiv:2304.12236

[hep-ex].

[24] K. Abe *et al.* (T2K Collaboration), “The T2K experiment,” *Nucl. Instrum. Methods Phys. Res. Sect. A* **659**, 106 (2011), arXiv:1106.1238 [physics.ins-det].

[25] D. Ayres *et al.* (NO ν A Collaboration), “The NO ν A Technical Design Report,” (2007), 10.2172/935497.

[26] K. Abe *et al.* (T2K), “Observation of Electron Neutrino Appearance in a Muon Neutrino Beam,” *Phys. Rev. Lett.* **112**, 061802 (2014), arXiv:1311.4750 [hep-ex].

[27] J. Zhang and J. Cao, “Towards a sub-percent precision measurement of $\sin^2\theta_{13}$ with reactor antineutrinos,” *JHEP* **03**, 072 (2023), arXiv:2206.15317 [hep-ex].

[28] P. Huber, M. Lindner, and W. Winter, “Simulation of long-baseline neutrino oscillation experiments with GLoBES (General Long Baseline Experiment Simulator),” *Comput. Phys. Commun.* **167**, 195 (2005), arXiv:hep-ph/0407333.

[29] P. Huber, J. Kopp, M. Lindner, M. Rolinec, and W. Winter, “New features in the simulation of neutrino oscillation experiments with GLoBES 3.0: General Long Baseline Experiment Simulator,” *Comput. Phys. Commun.* **177**, 432 (2007), arXiv:hep-ph/0701187.

[30] T. Alion *et al.* (DUNE), “Experiment Simulation Configurations Used in DUNE CDR,” (2016), arXiv:1606.09550 [physics.ins-det].

[31] A. Alekou *et al.*, “The European Spallation Source neutrino super-beam conceptual design report,” *Eur. Phys. J. ST* **231**, 3779 (2022), [Erratum: Eur.Phys.J.ST 232, 15–16 (2023)], arXiv:2206.01208 [hep-ex].

[32] P. Huber, M. Lindner, and W. Winter, “Superbeams versus neutrino factories,” *Nucl. Phys. B* **645**, 3 (2002), arXiv:hep-ph/0204352.

[33] P. Huber, M. Lindner, M. Rolinec, and W. Winter, “Optimization of a neutrino factory oscillation experiment,” *Phys. Rev. D* **74**, 073003 (2006), arXiv:hep-ph/0606119.

[34] A. Abusleme *et al.* (JUNO), “Sub-percent precision measurement of neutrino oscillation parameters with JUNO,” *Chin. Phys. C* **46**, 123001 (2022), arXiv:2204.13249 [hep-ex].

[35] G. Altarelli and F. Feruglio, “Discrete Flavor Symmetries and Models of Neutrino Mixing,” *Rev. Mod. Phys.* **82**, 2701 (2010), arXiv:1002.0211 [hep-ph].

[36] S. F. King and C. Luhn, “Neutrino Mass and Mixing with Discrete Symmetry,” *Rept. Prog. Phys.* **76**, 056201 (2013), arXiv:1301.1340 [hep-ph].

[37] S. T. Petcov, “Predicting the values of the leptonic CP violation phases in theories with discrete flavour symmetries,” *Nucl. Phys. B* **892**, 400 (2015), arXiv:1405.6006 [hep-ph].

[38] F. Costa and S. F. King, “Neutrino Mixing Sum Rules and the Littlest Seesaw,” *Universe* **9**, 472 (2023), arXiv:2307.13895 [hep-ph].